

Estimating methane emission durations using continuous monitoring systems

William S. Daniels,^{*,†} Meng Jia,[†] and Dorit M. Hammerling^{†,‡}

[†]*Department of Applied Mathematics and Statistics, Colorado School of Mines, Golden, Colorado, United States*

[‡]*Energy Emissions Modeling and Data Lab, The University of Texas at Austin, Austin, Texas, United States*

* E-mail: wdaniels@mines.edu

Abstract

We propose a method for estimating the duration of methane emissions on oil and gas sites, referred to as the Probabilistic Duration Model (PDM), that uses concentration data from continuous monitoring systems (CMS). The PDM probabilistically addresses a key limitation of CMS: non-detect times, or the times when wind blows emitted methane away from the CMS sensors (resulting in no detections). Output from the PDM can be used to bound the duration of emissions detected by snapshot measurement technologies, such as plane or satellites, that have limited ability to characterize emission duration due to the typically low temporal frequency (e.g. quarterly) at which they observe a given source. Linear regression indicates that the PDM has a bias of -4.9% ($R^2 = 0.80$) when evaluated on blinded controlled releases at the Methane Emissions Technology Evaluation Center (METEC), with 86.8% of estimates within a factor of 2x error from the true duration. We apply the PDM to a typical production site in the Appalachian Basin and use it to bound the duration of snapshot measurements.

We find that failing to account for CMS non-detect times results in underestimated emission durations of up to a factor of 65x (6,400%) on this site.

Keywords: methane, oil and gas, emission duration, emission frequency, continuous monitoring systems, greenhouse gas reporting

Synopsis: We develop a method to estimate methane emission durations using continuous monitoring systems and use it to bound the duration of snapshot measurements.

Introduction

Updates to the EPA’s Greenhouse Gas Reporting Program (GHGRP) will require oil and gas operators to report maintenance or abnormal methane emissions greater than 100 kg/hr starting in January 2025,¹ including emissions identified by third parties (e.g., Carbon Mapper²). With an increasing number of operators opting into voluntary aerial measurement campaigns and with new methane-focused satellites (e.g., MethaneSAT³) launched and soon providing publicly available data, the number of detected emissions meeting this reporting requirement is likely to increase.

A duration estimate is required for all emissions exceeding the 100 kg/hr reporting threshold so that a total mass of methane can be computed and reported under the EPA rule.¹ Infrequent snapshot measurements have limited ability to characterize emission duration due to the relatively low frequency at which they observe a given source. For example, an aerial measurement campaign measuring each site quarterly will only be able to bound emission start times at three month intervals, despite emissions potentially lasting for only a few hours or days.⁴ Satellites can provide more frequent measurements of a given source, but their current operational detection limits are greater than the 100 kg/hr threshold and cloud cover and surface albedo can also prevent detections.⁵

Higgins et al.⁶ propose methods for bounding emission durations using operational data, such as tank pressures from a Supervisory Control and Data Acquisition (SCADA) system.

They note that these methods will be useful to oil and gas operators for near-term regulatory compliance as measurement-based methods for estimating emission durations evolve, such as more frequent aerial sampling^{7,8} or supplementing snapshot measurements with continuous monitoring systems (CMS).⁹

Here we develop a method for estimating methane emission durations using point-in-space CMS. These sensor systems measure methane concentrations in near-real time at several fixed sensor locations, typically around the perimeter of oil and gas sites. In practice, 1 to 10 CMS sensors may be installed on a given site, depending on its complexity and the CMS technology vendor, with most production sites having around 4 sensors. For reference, Figure S2 in the Supporting Information (SI) file shows a typical oil and gas production site with point-in-space CMS sensors arranged around the perimeter.

There are often times when emitted methane is not blown toward any of the CMS sensors on a given site, which we will subsequently call “non-detect times.” During these times, the sensors will not record enhanced methane concentrations, making it incorrectly appear as if no emissions were occurring. In a simulated one-source scenario, Chen et al.¹⁰ find that non-detect times make up 78% of total time when using one CMS sensor and 45% of total time when using four CMS sensors. Non-detect times can cause a delay between emission onset and detection, ranging from 12 hrs on average using one sensor to 4.3 hrs on average using four sensors on a typical tank battery.¹¹

In this work, we propose the Probabilistic Duration Model (PDM), a method for directly estimating methane emission durations using CMS that accounts for non-detect times. We apply the PDM to CMS data collected during blinded controlled releases at the Methane Emissions Technology Evaluation Center (METEC) to demonstrate its practical feasibility. We then apply the PDM to CMS data collected on an oil and gas production site in the Appalachian basin as a part of the Appalachian Methane Initiative (AMI) and use it to bound the duration of snapshot aerial measurements.

Methods

The purpose of this section is threefold. First, we introduce a naive method for estimating emission durations that does not account for CMS non-detect times. Second, we introduce the PDM, which updates the duration estimates from the naive method by probabilistically accounting for non-detect times. Third, we describe the controlled release data used to evaluate the PDM.

Naive method for estimating emission durations

We use the clustering procedure from Daniels et al.¹² to create naive duration estimates. Specifically, we start by taking the minute-by-minute maximum across the concentration data from all CMS sensors installed on the site. This collapses the signal from each sensor into one time series while preserving the concentration enhancements that contain the most pertinent emission information.

We then apply the spike detection algorithm from Daniels et al.¹² to this maximum value time series, which uses a gradient-based method to identify sharply elevated concentration values, or spikes. We cluster all identified spikes into groups and background correct them by subtracting the average of the concentration values immediately preceding and following the groups. All other concentration values (that are not part of a group) are deemed background and are set to zero. The clustered groups of background-corrected enhancements are then taken as the naive emission events, referred to as the “naive events” throughout this article, and the “naive durations” are simply the lengths of these naive events.

The Probabilistic Duration Model (PDM)

The PDM is designed to improve the naive duration estimates described in the previous section by probabilistically accounting for CMS non-detect times. It does this by both extending the duration of naive events and combining neighboring naive events within a Monte Carlo

framework. As such, the PDM can be used to bound the duration of snapshot measurements by doing the following. First, identify the naive emission event that coincides with the snapshot measurement. Second, apply the PDM to this naive event to produce a distribution of possible durations. Third, take either the mean or maximum (if a conservative estimate is desired) of this distribution as the duration of the coinciding snapshot measurement.

The PDM is separated into four steps that are described in the following subsections. A visual summary of the model is provided in Figure S1 in the SI.

Characterize the naive events. We estimate an emission source and rate for each naive event using the method from Daniels et al.¹². This allows us to more accurately quantify the CMS non-detect times in the following step. Briefly, we estimate the emission source by comparing CMS concentration observations to forward simulated concentrations from each possible source. For each naive event, the estimated emission source is taken to be the source whose simulated concentrations most closely match the actual concentration observations (assessed using correlation). We estimate an emission rate for each naive event by minimizing mean square error between the simulated concentrations and the CMS concentration observations over a range of possible emission rates.

We use the Gaussian puff atmospheric dispersion model to forward simulate, which we describe in more detail in Section S2 of the SI and in Jia et al.¹³. Note that this step imposes the assumption that each naive emission event has only a single source.

Create information mask. We next identify the periods during which we expect the wind to blow emitted methane toward the sensors (the CMS detect times, or periods of “information”) and between the sensors (the CMS non-detect times, or periods of “no information”). We do so for each naive event by first simulating methane concentrations at the CMS sensor locations assuming the estimated source and rate for that naive event. We do this using the Gaussian puff atmospheric dispersion model and the actual wind data collected on the site. Similar to the procedure for identifying naive events, we then take the

minute-by-minute maximum of the simulated concentrations across all sensors on the site and apply the spike detection algorithm from Daniels et al.¹² to this maximum value time series. Clusters of identified spikes in the simulated concentrations are taken to be periods of information, as these are the times during which a simulated emission event created concentration enhancements at the sensor locations.

Compute probability of combining naive events. Occasionally, two or more consecutive naive events with the same source estimate are separated by periods of no information. There are two possible emission scenarios that could give rise to this situation: 1) the emission continued through the periods of no information, and 2) the emission stopped and started again during the periods of no information. We make the assumption that naive events separated in this manner are more likely to be from the same emission if their estimated rates are similar, regardless of the length of the no information period.

We define the probability, $\mathbb{P}_{i,j}$, of combining a given naive event, E_i , with another event, E_j , as

$$\mathbb{P}_{i,j} = 1 - \frac{|q_i - q_j|}{P_{95}(\mathbf{q}) - P_5(\mathbf{q})}, \quad (1)$$

where q_i and q_j are the estimated emission rates of naive events E_i and E_j , \mathbf{q} is a vector of estimated emission rates for all naive events, and $P_5()$ and $P_{95}()$ are functions returning the 5th and 95th percentiles. If E_j has a different source location estimate than E_i or is separated by a period of information, then we set $\mathbb{P}_{i,j} = 0$.

We do not use any operational data (e.g., SCADA data) when computing the probability of combining events, but we may investigate options for doing so in future work. We also note that estimating emission frequency is relatively straightforward once $\mathbb{P}_{i,j}$ has been computed for each pair of naive events. See Section S3 in the SI for details.

Create distribution of possible durations. We first identify the range of possible start and end times for each naive event without considering the probability of combining adjacent events. We do so using the following logic (see Figure S1 in the SI for a visual representation). If a naive event starts or ends during a period of information, then we assume that there is only one possible start or end time for that event. However, if a naive event starts at a transition from a period of no information to a period of information, then we assume that all times back to the previous period of information are equally likely to be the start time of that event. Similarly, if a naive event ends at a transition from a period of information to a period of no information, then we assume that all times up to the next period of information are equally likely to be the end time of that event.

We then use the following logic to create a distribution of possible durations for a given naive event, E_i . We refer to E_i as the event that the PDM is “applied to.” If E_i has zero probability of being combined with either adjacent event, then we sample uniformly from the range of possible start and end times for event E_i . If E_i has non-zero probability of being combined with one adjacent event, E_j , then we sample start times (if E_j occurs before E_i) or end times (if E_j occurs after E_i) with probability $\mathbb{P}_{i,j}$ from E_j and with probability $1 - \mathbb{P}_{i,j}$ from E_i . If E_i has non-zero probability of being combined with more than one adjacent event, then the procedure for sampling start and end times described above is applied recursively until an event, E_k , with $\mathbb{P}_{i,k} = 0$ is encountered. The differences in time between all combinations of sampled start and end times are taken as the distribution of possible durations for E_i . A point estimate of the event duration can be produced by taking the mean or maximum (if an upper bound is desired) of this distribution. Section S4 in the SI file contains details about the recursive sampling method.

Controlled release evaluations

We used data from three controlled release experiments to evaluate the PDM: 1) the 2022 Advancing Development of Emissions Detection (ADED) campaign conducted at METEC,¹⁴

2) the 2023 ADED campaign also conducted at METEC,¹⁵ and 3) the 2022 Stanford high emission rate release campaign conducted in Arizona.¹⁶ We used the ADED 2022 data in a non-blinded manner as a preliminary evaluation of the PDM. Section S5 in the SI contains a full description of this experiment and the PDM results.

We used the ADED 2023 data in a blinded manner to more robustly evaluate the PDM. This was done by splitting the author team into blinded and non-blinded groups. The blinded group ran the PDM on the CMS concentration data before accessing the controlled release truth data provided by METEC. The non-blinded group only shared the truth data with the blinded group after the PDM results were finalized, at which point we removed all duration estimates associated with multi-source releases. The PDM as currently implemented assumes a single source is emitting at a time, and so we only evaluate it during these scenarios. This experiment had 79 single-source controlled releases ranging from 0.1 to 7.1 kg/hr in size and 0.5 to 9.0 hrs in length. Methane concentration data for this evaluation came from 10 CMS sensors placed around the METEC facility. Section S6 in the SI contains a full description of this experiment.

We used the Stanford controlled release data to evaluate the PDM's performance on high rate emissions using the same blinding procedure as the ADED 2023 experiment. After filtering the controlled release data (described in Section S7 of the SI), this experiment contained 41 releases ranging from 9.0 to 1363.6 kg/hr, with 25 releases (61%) above the EPA's 100 kg/hr reporting threshold. Release durations ranged from 0.2 to 6.8 hrs. Methane concentration data for this evaluation came from 6 CMS sensors placed around a single release point.

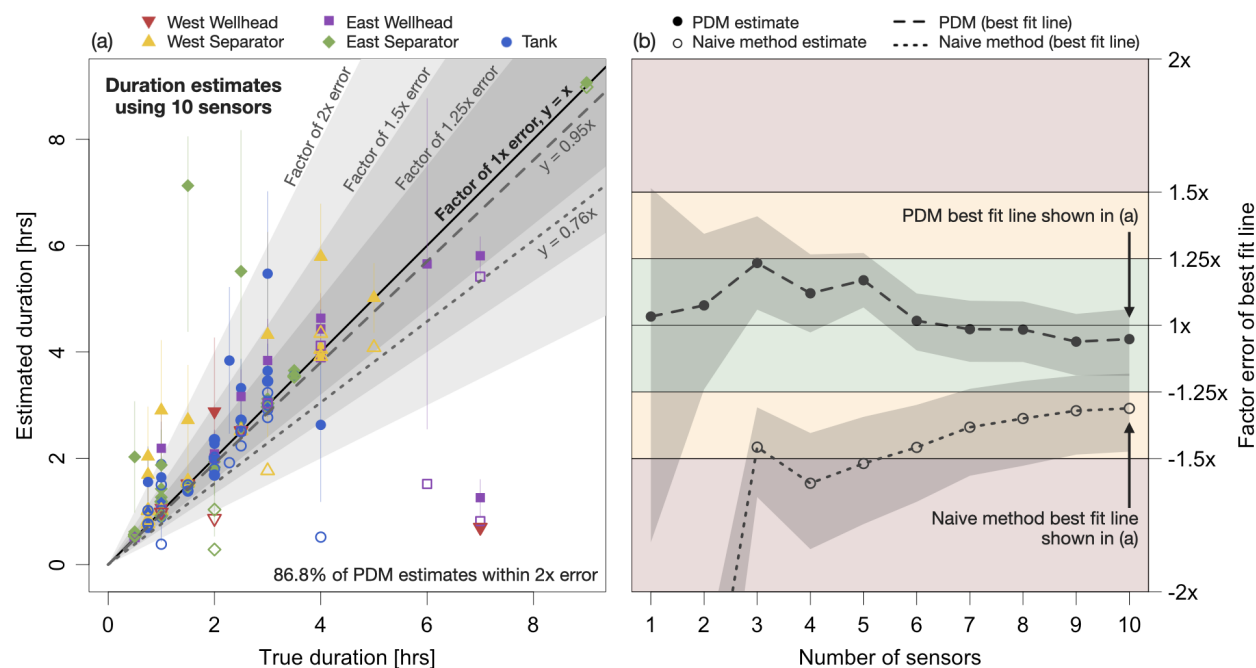


Figure 1: (a) Parity plot of estimated and true durations for the ADED 2023 controlled releases. Solid and empty points correspond to duration estimates from the PDM and naive methods, respectively, with vertical lines showing the 90% interval from the PDM and color showing the true emission source. Dashed and dotted lines show the best linear fit to the PDM and naive estimates, respectively. Gray shaded regions show three different error regimes. (b) Factor of over or underestimation by the best linear fit to the PDM and naive estimates using different numbers of sensors. Gray shaded regions show the 95% confidence interval on the estimated slope. Negative factor differences indicate underestimation. Colored sections correspond to the three error regimes in (a). Note that the vertical scale is limited to $[-2x, 2x]$ for visual clarity.

Results

Controlled release evaluations

Figure 1 summarizes the performance of the naive method and the PDM on the blinded ADED 2023 controlled releases. Figure 1(a) compares the duration estimates from both methods to the true durations using data from all 10 CMS sensors. We show duration estimates for events that coincide with a controlled release but not for false positive events, as there is no truth to compare these estimates against. The PDM estimates are taken to be the mean of the possible durations provided by the model.

The slope of the best fit line to the PDM estimates is 0.95 ($R^2 = 0.80$), indicating a slight tendency to underestimate durations. The naive method has a larger tendency to underestimate (slope = 0.76, $R^2 = 0.81$), which makes sense for two reasons. First, CMS non-detect times often result in naive events that start too late or end too early. The PDM is able to probabilistically extend these naive events by sampling start and end times from the periods of no information. Second, CMS non-detect times often separate concentration enhancements during a controlled release into multiple short naive events that each underestimate the duration of the release. The PDM is able to probabilistically recombine these short naive events, resulting in more accurate duration estimates in the presence of CMS non-detect times.

The PDM's benefit is more apparent when fewer CMS sensors are used, which is common in practice. To demonstrate this behavior, we recompute duration estimates using subsets of the 10 CMS sensors installed on the METEC site. For the n -sensor subset, we use only data from the n sensors that maximize detections by the CMS network based on wind data from the site. Figure 1(b) shows the degree of over or underestimation by the best fit line for the naive method and PDM under different sensor subsets. While the PDM best fit line stays relatively constant within a factor of 1.25x error, the naive method best fit line decreases steadily as fewer sensors are used. This makes sense, as there are more opportunities for wind to blow emitted methane between sensors that are spaced farther apart. A similar analysis using suboptimal n -sensor arrangements is provided in Section S8 in the SI.

Both the PDM and the naive method exhibit a larger tendency to underestimate when evaluated on the 2022 Stanford high emission rate releases. When all 6 CMS sensors are used, the slope of the best fit line to the PDM estimates is 0.64 ($R^2 = 0.56$, factor error = -1.56x) and the slope of the best fit line to the naive estimates is 0.53 ($R^2 = 0.63$, factor error = -1.88x). Almost all cases of extreme underestimation by the naive method (factor error less than -2x) were the result of one controlled release being separated into two short naive events by gaps in the concentration enhancements. Unlike the ADED 2022 and 2023

experiments, the PDM did not recombine any of these naive event pairs, as almost all of them were erroneously separated by periods of information (resulting in zero probability of being combined). A full discussion of what could have caused errors in the information mask is provided in Section S6 in the SI. When these naive event pairs are removed, the slope of the best fit line to the PDM estimates is 1.02 ($R^2 = 0.74$, factor error = 1.02x) and the slope of the best fit line to the naive estimates is 0.82 ($R^2 = 0.80$, factor error = -1.22x). This finding underscores the need for high fidelity atmospheric dispersion models in methane emissions modeling.

Real site case study

We apply the PDM to CMS data collected from August 21 to October 31, 2023 on an oil and gas production site in the Appalachian basin as a part of the Appalachian Methane Initiative (AMI). This site was selected for a case study because it had the simplest configuration among AMI sites instrumented with CMS and was therefore most likely to satisfy the single-source assumption of the PDM. Figure 2(a) shows a schematic of this site, with the locations of CMS sensors and potential emission sources marked. Figure 2(b) shows the range of naive duration estimates and PDM estimates across all identified emission events on the site. PDM estimates are taken as the mean of possible durations provided by the model. Section S3 in the SI lists the emission frequency estimates for this site.

We use the PDM to bound the duration of a hypothetical snapshot measurement on this site, as no actual snapshot measurements were taken while the CMS were deployed. Figure 3(a) shows the time of this hypothetical measurement and the overlapping CMS data. Without accounting for non-detect times, the duration of naive event III could be taken as the duration estimate for the coinciding snapshot measurement. However, there are multiple naive events also localized to Wellheads 1 surrounding event III, many of which are separated by periods of no information. Taking this into account via the PDM results in a distribution of possible emission durations for event III, shown in Figure 3(b), and

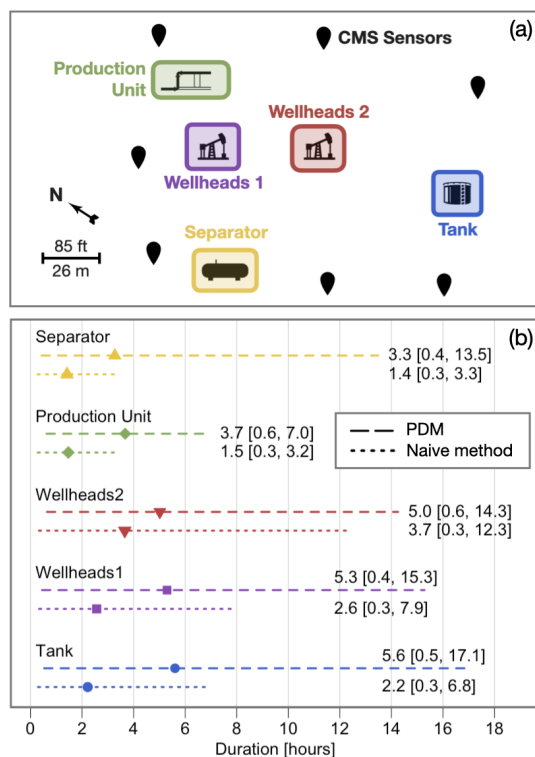


Figure 2: (a) Schematic of the oil and gas production site used as a case study in this article. (b) Summary of the duration estimates on this site. The left- and right-most points of the horizontal lines show the 5th and 95th percentiles of the duration estimates across all emission events. The symbols show the average duration estimate. These values are also printed on the figure in the format: mean [5th percentile, 95th percentile].

hence a distribution of possible durations for the coinciding snapshot measurement. The naive duration estimate (1.9 hrs) is shorter than the mean (8.3 hrs) and maximum (11.5 hrs) estimates from the PDM by a factor of 4.4x and 6.1x, respectively. This underestimation would impact the estimate of total emitted methane to the same degree.

Finally, to probe the extent of possible underestimation by the naive method, we repeat our analysis on this site for all possible snapshot measurement times. The largest instance of underestimation was by a factor of 36.4x and 64.8x compared to the mean and maximum estimate from the PDM, respectively. More details about this case study, including two additional hypothetical snapshot measurement examples, are given in Sections S9-S11 of the SI file.

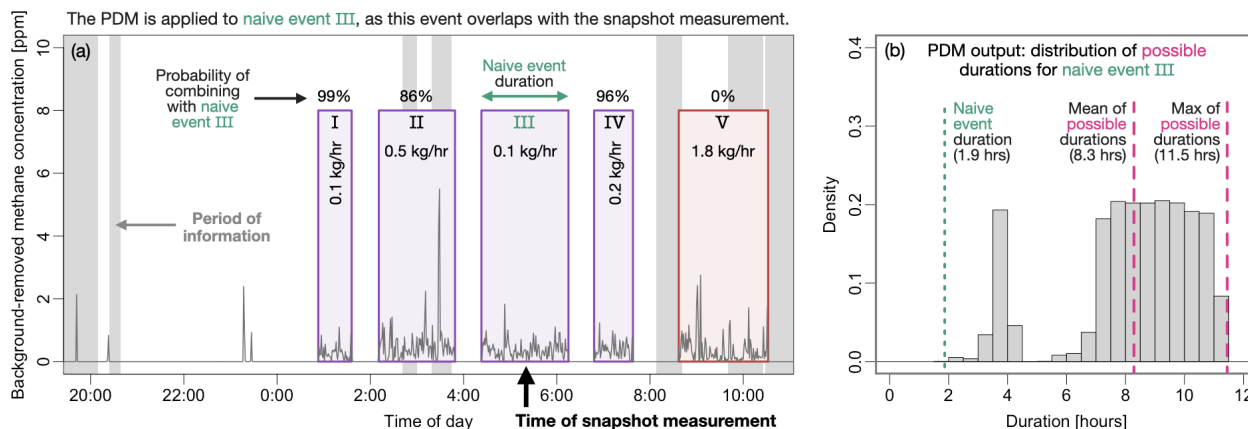


Figure 3: (a) Example snapshot measurement (time indicated by black arrow) and the overlapping CMS concentration data (spanning September 27, 2023 at 8:00pm to September 28, 2023 at 10:30am). Enumerated boxes show the naive events, with color indicating the source estimate (color corresponds to the schematic in Figure 2(a)). Gray shaded regions mark periods of information. Percents indicate the probability of combining each event with the naive event that overlaps the snapshot measurement. (b) Distribution of possible durations from the PDM for naive event III and hence the overlapping snapshot measurement.

Discussion

This study has revealed a number of important considerations for aerial measurement campaigns and the finalized EPA rule coming into effect in January 2025:

1. CMS can complement snapshot measurements by bounding the duration of detected emissions. Aerial measurements alone have limited ability to bound the duration of intermittent emission events, as measurement campaigns are often performed only quarterly or yearly.
2. If ignored, CMS non-detect times can result in significant underestimation of emission duration, to the point where the use of CMS could unintentionally circumvent a majority of the methane fees associated with large emissions. As such, addressing CMS non-detect times is critical for accurate duration estimates.
3. We propose a method for estimating emission durations using CMS that probabilistically accounts for non-detect times. The benefit of this method is especially apparent

when only a small number of sensors are installed on a given site, which is common in practice and results in limited coverage.

Current commercially available CMS solutions have large quantification errors on controlled releases,^{14–16} but their detection capabilities show promise, especially for larger emissions.¹⁶ Therefore, while quantification capabilities evolve, CMS can complement snapshot measurements by bounding the duration of detected emissions.

Finally, we note a number of limitations of the PDM as currently implemented. First, it assigns zero probability of combining adjacent naive events if their source estimates are different, meaning that errors in localization estimates can propagate to errors in duration estimates. Second, periods of information are subject to errors in the Gaussian puff dispersion model, which can result in naive events that occur during periods of no information (e.g., naive events I, III, and IV in Figure 3). Third, the PDM assumes a single emission source for all emission events. The ability to localize multi-source emissions will be necessary for accurate CMS-based duration estimates on complex sites where this assumption breaks down, and methods to do so are currently under development.

Funding

This work was funded by the Energy Emissions Modeling and Data Lab (EEMDL) through a grant from the Department of Energy (DOE) designed to facilitate data analysis for the Appalachian Methane Initiative (AMI).

Competing Interests

The authors have no competing interests to declare.

Acknowledgement

The authors thank the participating oil and gas operators and measurement technology vendors, in particular Project Canary and Qube Technologies, for generously donating their measurement data for use in algorithm development. The authors also thank Dr. Shuting (Lydia) Yang, Dr. Shannon Stokes, Dr. Jiayang (Lyra) Wang, SLR International Corporation, and the other members of the Appalachian Methane Initiative (AMI) scientific team for logistic and scientific support.

Supporting Information Available

The following files are available free of charge.

- Supporting Information: Contains additional details about the controlled release experiment and the case study.
- Code and data are available at: <https://github.com/wsdaniels/CMS-durations>

References

- (1) U.S. Environmental Protection Agency. *Greenhouse Gas Reporting Rule: Revisions and Confidentiality Determinations for Petroleum and Natural Gas Systems*; Final Rule 89 FR 42062, 2024; pp 42062–42327, <https://www.federalregister.gov/d/2024-08988>.
- (2) Carbon Mapper Data. 2024; <https://data.carbonmapper.org>.
- (3) MethaneSAT Data. 2024; <https://www.methanesat.org/data/>.
- (4) Wang, J. L.; Daniels, W. S.; Hammerling, D. M.; Harrison, M.; Burmaster, K.; George, F. C.; Ravikumar, A. P. Multiscale Methane Measurements at Oil and Gas

- Facilities Reveal Necessary Frameworks for Improved Emissions Accounting. *Environmental Science & Technology* **2022**, *56*, 14743–14752, <https://doi.org/10.1021/ACS.EST.2C06211>.
- (5) Sherwin, E. D.; El Abbadi, S. H.; Burdeau, P. M.; Zhang, Z.; Chen, Z.; Rutherford, J. S.; Chen, Y.; Brandt, A. R. Single-blind test of nine methane-sensing satellite systems from three continents. *Atmospheric Measurement Techniques* **2024**, *17*, 765–782, <https://doi.org/10.5194/amt-17-765-2024>.
- (6) Higgins, S.; Hecobian, A.; Baasandorj, M.; Pacsi, A. P. A Practical Framework for Oil and Gas Operators to Estimate Methane Emission Duration Using Operational Data. *SPE Journal* **2024**, *29*, 2763–2771, <https://doi.org/10.2118/219445-PA>.
- (7) Schissel, C.; Allen, D. T. Impact of the High-Emission Event Duration and Sampling Frequency on the Uncertainty in Emission Estimates. *Environmental Science & Technology Letters* **2022**, *9*, 1063–1067, <https://doi.org/10.1021/acs.estlett.2c00731>.
- (8) Cardoso-Saldaña, F. J. Tiered Leak Detection and Repair Programs at Simulated Oil and Gas Production Facilities: Increasing Emission Reduction by Targeting High-Emitting Sources. *Environmental Science & Technology* **2023**, *57*, 7382–7390, <https://doi.org/10.1021/acs.est.2c08582>.
- (9) Daniels, W. S.; Wang, J. L.; Ravikumar, A. P.; Harrison, M.; Roman-White, S. A.; George, F. C.; Hammerling, D. M. Toward Multiscale Measurement-Informed Methane Inventories: Reconciling Bottom-Up Site-Level Inventories with Top-Down Measurements Using Continuous Monitoring Systems. *Environmental Science & Technology* **2023**, *57*, 11823–11833, <https://doi.org/10.1021/acs.est.3c01121>.
- (10) Chen, Q.; Schissel, C.; Kimura, Y.; McGaughey, G.; McDonald-Buller, E.; Allen, D. T. Assessing Detection Efficiencies for Continuous Methane Emission Monitoring Systems

- at Oil and Gas Production Sites. *Environmental Science & Technology* **2023**, *57*, 1788–1796, <https://doi.org/10.1021/acs.est.2c06990>.
- (11) Chen, Q.; Kimura, Y.; Allen, D. Determining times to detection for large methane release events using continuously operating methane sensing systems at simulated oil and gas production sites. *ChemRxiv* **2023**, <https://doi.org/10.26434/chemrxiv-2023-p81fk>.
- (12) Daniels, W. S.; Jia, M.; Hammerling, D. M. Detection, localization, and quantification of single-source methane emissions on oil and gas production sites using point-in-space continuous monitoring systems. *Elementa: Science of the Anthropocene* **2024**, *12*, 00110, <https://doi.org/10.1525/elementa.2023.00110>.
- (13) Jia, M.; Daniels, W. S.; Hammerling, D. M. Comparison of the Gaussian plume and puff atmospheric dispersion models for methane modeling on oil and gas sites. *ChemRxiv* **2023**, <https://doi.org/10.26434/chemrxiv-2023-hc95q-v2>.
- (14) Bell, C.; Ilonze, C.; Duggan, A.; Zimmerle, D. Performance of Continuous Emission Monitoring Solutions under a Single-Blind Controlled Testing Protocol. *Environmental Science & Technology* **2023**, *57*, 5794–5805, <https://doi.org/10.1021/acs.est.2c09235>.
- (15) Ilonze, C.; Emerson, E.; Duggan, A.; Zimmerle, D. Assessing the Progress of the Performance of Continuous Monitoring Solutions under a Single-Blind Controlled Testing Protocol. *Environmental Science & Technology* **2024**, *58*, 10941–10955, <https://doi.org/10.1021/acs.est.3c08511>.
- (16) Chen, Z.; El Abbadi, S. H.; Sherwin, E. D.; Burdeau, P. M.; Rutherford, J. S.; Chen, Y.; Zhang, Z.; Brandt, A. R. Comparing Continuous Methane Monitoring Technologies for High-Volume Emissions: A Single-Blind Controlled Release Study. *ACS ES&T Air* **2024**, <https://doi.org/10.1021/acsestair.4c00015>.

TOC Graphic

